Adsorption, Exchange, and Oxidation of Formaldehyde on Gold: A Radiotracer Study

M. V. ten Kortenaar,[†,‡] Z. I. Kolar,[*,†] J. J. M. de Goeij,[†] and G. Frens[‡]

Interfaculty Reactor Institute, Delft University of Technology, Mekelweg 15, 2629 JB, Delft, The Netherlands, and Laboratory of Physical Chemistry, Delft University of Technology, Julianalaan 136, 2628 BL Delft, The Netherlands

Received April 19, 2001. In Final Form: May 31, 2002

The adsorption, exchange, and oxidation of formaldehyde have been studied on gold at various potentials, temperatures, concentrations, and pH values by voltammetry and the radiotracer thin-gap method and compartmental analysis. Two adsorption rates were identified in the overall adsorption process at the open circuit potential (OCP): a rapid physisorption and a slow chemisorption. Compartmental analysis of the adsorption kinetic data revealed that the physisorption and chemisorption steps proceed in a catenary (serial), reversible fashion. Approximately linear adsorption isotherms were obtained under most conditions, implying that the Gibbs free energy of the reaction depends only a little on the potential, temperature, and pH (the activation energy was previously seen to be strongly affected by these variables). The strong dependence of the quantity of species adsorbed on the formaldehyde concentration in the solution and the invariance of the adsorption isotherms with increasing potentials support the view that potential gradients on the solution side are more important in the adsorption of species than the potential of the electrode itself. At pH 13, the kinetics of the electro-oxidation of formaldehyde is approximately first order both in the concentration of formaldehyde and in the quantity of species adsorbed at the gold surface. The overall rate of the reaction is determined by chemisorption of the enolate anion at low potentials, by desorption of formate at medium potentials, and by diffusion of reactants and products at the highest potentials. Free energies of adsorption (ΔG_a) ranged between −29.1 and −25.3 kJ mol^{-1}, heats of adsorption (ΔH_a) between −93.9 and −9.0 kJ mol^{-1}, and entropies of adsorption (ΔS_a) between −0.2 and 0.1 kJ mol^{-1}.

Introduction

As semiconductor process technology advances toward 100 nm silicon geometries within 5 years, growing interest is noticed in selective electroless metal deposition for microelectronic applications.[1−3] Kinetic control of the selective deposition processes has nevertheless remained an empirical matter restricting the application of electroless copper deposition relative to electrolytic copper deposition.[3,4] Attempts to narrow the gap have resulted in numerous reports on the electro-oxidation of formaldehyde on various catalytic metals.[4−10] Most reports have addressed the mechanistic aspects of the reaction although little effort has been expended to come to kinetic descriptions for the control of practical deposition processes.[11] To arrive at these descriptions, quantitative knowledge on the reaction kinetics of the reducing agents used in electroless plating is desired.[1,11]

Recently, we have applied electrochemical impedance spectroscopy (EIS) to study the electro-oxidation of formaldehyde on gold in alkaline solutions.[11] A double-layer structure was constructed from the results which described the electrostatic and kinetic features of the electro-oxidation reaction in a qualitative fashion. The view was specified by voltammetry and differential electrochemical mass spectrometry (DEMS) with the determination of the apparent activation energies (E_a) and the kinetic isotope effects (KIE) of the reaction.[12] The various results were in line with the following mechanism:

$$CH_2(OH)_2 + OH^- \leftrightarrow CH_2OHO^- + H_2O \quad (\textit{Ionization}) \quad \text{(I)}$$

$$CH_2OHO^- \leftrightarrow CH_2OHO^-_{surface} \quad (\textit{Diffusion to surface}) \quad \text{(II)}$$

$$CH_2OHO^-_{surface} \leftrightarrow CH_2OHO^-_{phys} \quad (\textit{Physisorption}) \quad \text{(III)}$$

$$CH_2OHO^-_{phys} \leftrightarrow {}^{\bullet}CHOHO^-_{chem} + {}^{\bullet}H_{chem} \quad (\textit{Chemisorption}) \quad \text{(IV)}$$

$${}^{\bullet}CHOHO^-_{chem} + OH^- \rightarrow HCOO^- + H_2O + e^- \quad (\textit{Oxidation, Desorption}) \quad \text{(V)}$$

Atomic hydrogen formed in step IV may react to molecular hydrogen or to water:

$${}^{\bullet}H_{chem} + {}^{\bullet}H_{chem} \rightarrow H_2 \quad (\textit{H}_2\textit{ evolution}) \quad \text{(VI)}$$

$${}^{\bullet}H_{chem} + OH^- \rightarrow H_2O + e^- \quad (\textit{Oxidation, desorption}) \quad \text{(VII)}$$

* Corresponding author. E-mail: kolar@iri.tudelft.nl.
† Interfaculty Reactor Institute.
‡ Laboratory of Physical Chemistry.

(1) Paunovic, M. In *Electrochemistry in Transition*; Murphy, O. J., Srinivasan, S., Conway, B. E., Eds.; Plenum Press: New York, 1992; Chapter 30, p 479.
(2) Manders, B. S.; Laat, W. T. F. M. de. *The Electrochemical Meeting Abstracts*, Vol. 96−1; Los Angeles, 1996; p 191.
(3) Shacham-Diamand, Y. *J. Micromech. Microeng.* **1991**, *1*, 66.
(4) West, A. C.; Cheng, C. C.; Baker, B. C. *J. Electrochem. Soc.* **1998**, *145*, 3070.
(5) Beltowska-Brzezinska, M. *Electrochim. Acta* **1985**, *30*, 1193.
(6) Beltowska-Brzezinska, M. *J. Electroanal. Chem.* **1985**, *187*, 167.
(7) Enyo, M. *J. Appl. Electrochem.* **1985**, *15*, 907.
(8) Adzic, R. R.; Avramov-Ivic, M. L. *J. Electroanal. Chem.* **1982**, *134*, 177.
(9) Avramov-Ivic, M. L.; Anastasijevic, N. A.; Adzic, R. R. *Electrochim. Acta* **1990**, *35*, 725.
(10) Burke, L. D.; O'Dwyer, K. J. *Electrochim. Acta* **1990**, *11*, 1829.
(11) Kortenaar, M. V.; Tessont, C.; Kolar, Z. I.; Weijde, H. van der. *J. Electrochem. Soc.* **1999**, *14*, 2146.
(12) Kortenaar, M. V.; Kolar, Z. I.; Goeij, J. J. M. de.; Frens, G. *J. Electrochem. Soc.* **2001**, *148*, 1.

10.1021/la010572c CCC: $22.00
Published on Web 12/02/2002

The present paper uses this mechanism to discuss the adsorption, exchange, and oxidation kinetics of formaldehyde on gold at various temperatures, pH's, concentrations, and potentials. Data have been collected by voltammetry and the radiotracer thin-gap technique.[13] A kinetic−thermodynamic picture of the reaction is pursued which may serve as a springboard for a kinetic description of simple electroless deposition processes.[11] The insight in the kinetics of the reaction obtained from this work is to be used in the discussion of the electrooxidation of formaldehyde on other transition metals in a next report.[14]

Experimental Section

(I) Materials and Equipment. Solutions were prepared from chemicals of analytical grade (Sigma, Belgium) and milli-Q water (Millipore, 18.2 MΩ·cm^{-1}). Both paraformaldehyde and deuterated paraformaldehyde (D quantity in CD_2O > 99%, Thamer diagnostica, Uithoorn, The Netherlands) were dissolved in water by ultrasonic vibration. Solutions contained at least 99% CH_2O, as determined iodometrically.[11,12] No attempts were made to further purify the solution, as practical formaldehyde solutions used in electroless plating also contain small amounts of methanol and formate due to the Canizzaro reaction.[15,16] The [^{14}C]-labeled CH_2O (ICN, The Netherlands) used for the radiotracer adsorption and exchange studies had a specific activity of 1.99 GBq mmol^{-1} and a radioactive concentration of 0.7 GBq mL^{-1}, respectively. The [^{35}S]-labeled Na_2SO_4 (ICN, The Netherlands) used for the determination of the gap thickness was carrier free (specific activity about 50 TBq mol^{-1}).

Disk-shaped polycrystalline gold electrodes (thickness 5 mm, diameter 11.5 mm, 99.99%, Goodfellow, England) were optically cut and polished using 1.0 μm and 0.25 μm diamond paste. A platinum electrode and a Hg/Hg_2SO_4(sat. K_2SO_4) electrode were used as counter electrode and reference electrode, respectively. The gold electrodes were pretreated by rinsing with 0.1 M $HClO_4$, followed by potentiodynamic cycling between −1.3 and 0.4 V vs Hg/Hg_2SO_4 in 0.1 M NaOH. Cycling was continued until signals were reproducible and indicative for clean gold.[12,17]

Voltammetry and radiotracer studies were carried out using a scanning potentiostat (EG&G, type 362) and a double-wall glass cell which was connected to a thermostat.[13,18] The bottom of the cell consisted of a glass scintillator embedded in a ceramic disk covered by a protecting, transparent polyethylene film. Light signals were detected using a photomultiplier tube (PMT, Thorn EMI, type B2F/RFI), a power supply (EG&G Ortec, type 478), an amplifier (Canberra, type TSCA, 2015A), and a multichannel analyzer as the data collector (Tracor Northern, type 7200). The high voltage supply to the PMT operated at 1500 V during all measurements. Nitrogen was bubbled through the cell in each experiment at ∼3 bubbles per second, as counted by the eye.

(II) Radiotracer Thin-Gap Method. The thin-gap method has been described in detail elsewhere, but as slightly different procedures were followed, it is briefly summed up.[13] A flat electrode is pressed against the polyethylene foil (thickness 1 mm) and the glass scintillator in the bottom of the cell. The scintillator converts β-radiation of ^{14}C in the radiolabeled molecules, adsorbed on the electrode and present in the solution layer between the electrode and the foil-covered scintillator, into electric pulses which are amplified and collected. The amount of

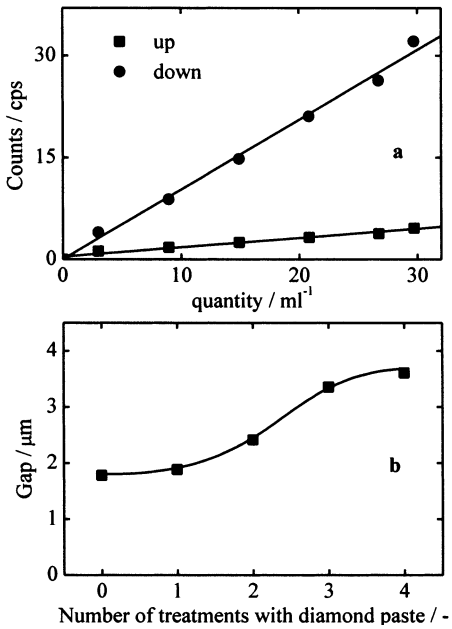

Figure 1. System responses upon increasing concentrations of [^{35}S]Na_2SO_4 in the solution containing 0.1 M $HClO_4$. The electrode potential was held at −0.6 V vs Hg/Hg_2SO_4 (a). Gap thickness as a function of the amount of scouring treatments (b).

species adsorbed at the electrode can be obtained from eq 1[19]

$$\Gamma = \frac{10^{-3} N_{ads} C}{N_s^{up} \mu_s R F_b \exp(-\mu_s x)} \quad (1)$$

where Γ (mol cm^{-2}) is the concentration of adsorbed species at the surface, N_{ads} (cps) is the net count rate from the adsorbate on the electrode surface counted when the electrode is in the "down" position, N_s^{up} (cps) is the counting rate from the solution and the adsorbate at the polyethylene foil counted when the electrode is in the "up" position, C (mol dm^{-3}) is the concentration of adsorbate in the bulk solution, μ_s is the linear absorption coefficient of β-radiation in water (300 cm^{-1} for ^{14}C, 256 cm^{-1} for ^{35}S at 295 K), R (unitless) is the roughness factor of the electrode surface, x (cm) is the gap thickness between the electrode and the foil on the glass scintillator, and F_b (unitless) is the backscattering factor, which can be obtained from eq 2

$$F_b = 2 - \exp[-Z/40] \quad (2)$$

where Z is the atomic number ($Z \geq 4$). F_b amounts to 1.86 for gold.[17,19]

The gap thickness, x, must be calibrated under conditions when no adsorption occurs.[18,19] As these conditions did not apply to the formaldehyde−gold system (see below), the gap thickness was obtained by measuring the up and down signals for the gold−sodium sulfate system (^{35}S has a β-energy spectrum comparable to that of ^{14}C).[19,20] Increasing amounts of a radioactive [^{35}S]-labeled Na_2SO_4 solution (radioactive concentration 104 MBq mL^{-1}) were injected into 10 mL of 0.1 M $HClO_4$ at −0.6 V vs Hg/Hg_2SO_4. Signals were recorded in the up and in the down positions (Figure 1a). The gap thickness was calculated from eq 3[19,20]

$$N_s^d/N_s^{up} = [1 - \exp(-\mu_s x)][1 + (F_b - 1)\exp(-\lambda x)] \quad (3)$$

where N_s^d is the counting rate (cps) in the down position, the ratio N_s^d/N_s^{up} is called the squeeze efficiency, and λ is the linear

(13) Krauskopf, E. K.; Chan, K.; Wieckowski, A. *J. Phys. Chem.* **1987**, *91*, 2327.
(14) Kortenaar, M. V.; Kolar, Z. I.; Goeij, J. J. M. de; Frens, G. To be submitted to *Langmuir*.
(15) Walker, J. F. *Formaldehyde*, 3rd ed.; Reinhold Publ. Corp.: New York, 1964; p 214.
(16) Meerakker, J. E. M.; van den Scholten, E. *Ber. Bunsen-Ges. Phys. Chem.* **1989**, *93*, 786.
(17) Kolics, A.; Thomas, A. E.; Wieckowski, A. *J. Chem. Soc., Faraday Trans.* **1996**, 92, 3727.
(18) Thomas, A. E.; Sung, Y. E.; Gamboa-Aldéco, M.; Franaszczuk, K.; Wieckowski, A. *J. Electrochem. Soc.* **1995**, *142*, 476.
(19) Szklarczyk, M.; Smolinski, S.; Sobkowski, J. *Electrochim. Acta* **1994**, *39*, 1903.
(20) Zelenay, P.; Rice-Jackson, L. M.; Wieckowski, A. *J. Electroanal. Chem.* **1990**, *283*, 389.

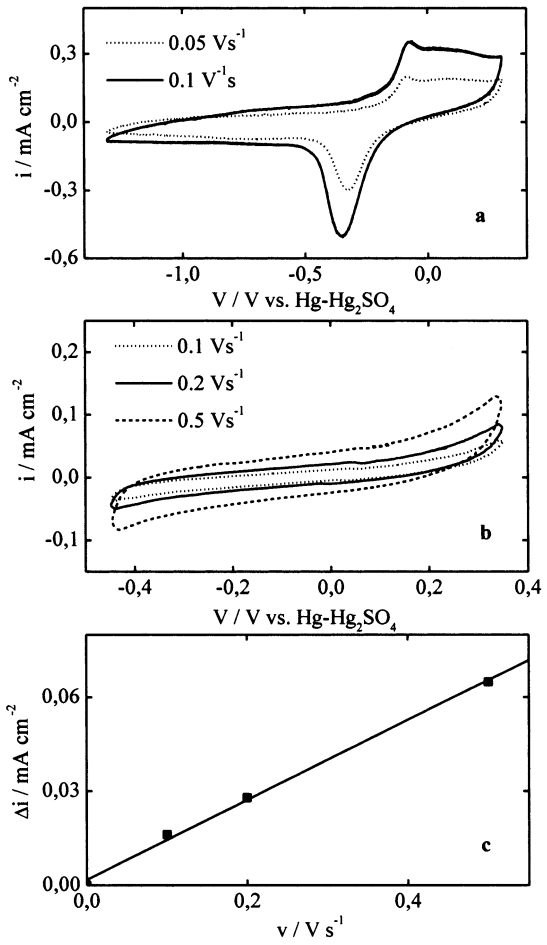

Figure 2. Cyclic voltammograms obtained in 0.1 M NaOH for the gold electrode used in the adsorption experiments (a). Cyclic voltammograms obtained for the same electrode in 0.1 M $NaClO_4$ (b). Dependence of the capacitive current on the scan rate (c).

absorption coefficient (cm^{-1}) in water for the backscattered β-radiation, which can be obtained from eq 4:[19]

$$\lambda = 225\mu_s/(106 + Z) \qquad (4)$$

As adsorption of formaldehyde on the polyethylene foil could eclipse the signal originating from the electrode surface, it was examined by liquid scintillation counting. Five pieces of polyethylene film were dipped for different periods of time into 100 mL of a radioactive, [^{14}C]-labeled formaldehyde and 0.1 M NaOH and 10^{-2} M CH_2O containing solution (radioactive concentration: 0.04 MBq mL^{-1}). Then, pieces were thoroughly rinsed with 0.1 M NaOH, dipped into 10 mL of Ultima Gold XR scintillation cocktail (Packard), and counted using a liquid scintillation counter (Packard, type Tricarb 2750/LL). As signals obtained did not increase at longer times, and as they did not differ from those for pieces which were not exposed to the radioactive solution, it was assumed that no significant irreversible adsorption of formaldehyde on the film had occurred.

Repeated scouring of the optically cut electrodes induced a roughening of the gold surface, and the gap thickness was determined as a function of the amount of scouring treatments (Figure 1b). The electrodes treated twice with 0.25 μm diamond paste yielded the most reproducible voltammograms, indicative for clean gold (Figure 2a), and it was decided to conduct all measurements with these electrodes.[17] Moreover, an attempt was made to derive the roughness factor of the electrode by comparing the double layer capacitances of the gold electrode, obtained from the cyclic voltammograms recorded in 0.1 M $NaClO_4$ (Figure 2b), with the minimum value of 22 μF cm^{-2} reported for single crystalline gold (111) surfaces (corresponding with a roughness factor of 1).[21] The linear dependence of the current with increasing scan rates at −0.48 V vs Hg/Hg_2SO_4 pointed toward the capacitive character of the current (Figure 2c) although the current density was not entirely independent of the potential (no conditions were found where this was the case). Still, the double layer capacitance was derived by using $i = Cv$, where v is the scan rate (in V s^{-1}), C is the capacitance (in F cm^{-2}), and i is the current density (F cm^{-2}). It yielded a value of 65.9 μF cm^{-2} and a roughness factor of 3.0.[21] As the latter was in agreement with the value of 3.3 obtained for a gold electrode pretreated in a similar way (at a potential where the current density did not depend on the potential), and as the main focus of the adsorption study was laid on the differences in response to the various solutions rather than on the detailed elucidation of absolute quantities (see below), the value of 3.0 was assumed correct.[14]

Table 1. Solutions and Conditions Used for the Adsorption and Exchange Experiments

proc	T/ °C	$[CH_2O]/10^{-3}$ mol dm^{-3}	[NaOH]/ mol dm^{-3}	$[CD_2O]/10^{-3}$ mol dm^{-3}	OCP/V vs Hg/Hg_2SO_4
1	23	10	0.1		−1.04
2	23		0.1	10	−1.01
3	38	10	0.1		−1.07
4	53	10	0.1		−1.10
5	23	10	0.005		−0.46
6	23	10	1.0		−1.07
7	23	0.17	0.1		−0.97

After the various constants of eq 1 were determined, the net counting rates originating from the adsorbate on the electrode, N_{ads}, were obtained by first collecting counts when the electrode was in the down position. Then, both the background signal, measured prior to the injection of the radiolabeled species into the cell, and the signal originating from the radioactive solution in the thin layer were subtracted. The latter was calculated from the squeeze efficiency obtained for the gold−sodium sulfate system.[20] Each value given below was an average of six data points.

(III) Measurement Procedures. *Adsorption Kinetics.* The adsorption kinetics of formaldehyde on gold was studied by first injecting 9 mL of 0.1 M NaOH into the glass cell with the gold electrode held in the up position. The electrode was then pressed down and 1.1 mL of a [^{14}C]-labeled formaldehyde, 0.1 M NaOH, and 10^{-2} M CH_2O containing solution (radioactive concentration: 3.4 MBq mL^{-1}) was injected into the cell and homogenized by air bubbling. When neither adsorption nor diffusion of the labeled formaldehyde into the trapped solution layer had occurred, as revealed by the constant, low counting rate of the system, the electrode was lifted. The electrode was then held in the up position until both complete homogenization of the labeled formaldehyde in the thin gap and adsorption of formaldehyde onto the electrode had occurred. Complete homogenization conditions were deduced from the unchanged up and down signals in the situation where no adsorption occurred (i.e. the gold-sulfate system).[20] Adsorption was seen from the increased signal when the electrode had been pressed down. The procedure of holding up the electrode for a fixed period of time, pressing it down, and measuring was repeated for the gold−formaldehyde system until the down signal remained constant.

Exchange Kinetics. When adsorption of molecules at the gold surface was completed, the electrode was pressed down and the solution was pumped out. The trapped solution had thereby remained in the gap, as revealed by the unchanged response of the system. Then, 10 mL of a solution containing CH_2O and NaOH at the same concentrations as those used for the adsorption experiment (see above) was injected into the cell. The electrode was repeatedly held in the up position for different periods of time and pressed down until the down signal remained constant. The adsorption and exchange kinetics were studied at the open circuit potential (OCP) in solutions as listed in Table 1.

Potential Dependence. The dependence of the adsorption of formaldehyde on the potential applied was studied by first

(21) Shi, Z.; Lipkowski, J.; Gamboa, M.; Zelenay, P.; Wieckowski, A. *J. Electroanal. Chem.* **1994**, *366*, 317.

injecting 100 μL of a [^{14}C]-labeled formaldehyde solution (radioactive concentration 37 MBq mL^{-1}) into 10 mL of 0.1 M NaOH. Then, the up and down signals were measured, first at the OCP, then at the most negative potential of interest, and then at higher potentials. Data were collected at each potential when counting rates remained constant. After stepping to the highest potential, the electrode was held at the OCP for 20 min and the concentration was raised by injecting known quantities of formaldehyde into the cell. Again, the quantity of the electrode was measured at different potentials.

Temperature Dependence. The adsorption at different temperatures was studied by raising the temperature stepwise from room temperature to ~55 °C while measuring the counting rates. After completing the measurements at the OCP, the potential was stepped to 300 mV versus the OCP (see Table 1). The count rates were then measured again, first at higher temperature and then at lower temperatures.

(IV) Compartmental Analysis. To describe the overall adsorption and exchange process at the OCP in a quantitative fashion, a compartmental analysis was carried out:[22,23] The overall adsorption process was imagined by various (pseudo)stable states, called compartments, which were interconnected by mass flows of formaldehyde. The rates of the formaldehyde mass flows were assumed to obey first-order kinetics with rate constants being independent of both the formaldehyde concentration in the solution and the surface coverage. Moreover, the concentration of formaldehyde (exchange experiments) and its specific activity (adsorption experiments) were assumed constant in the compartments during each measurement.[22,23] Derivation of the most appropriate compartmental model was performed by first determining the minimum amount of compartments required to describe the data properly. Then, the sets of differential equations associated with each model were derived and fitted to the data (first to the adsorption kinetic curves and then to the exchange kinetic curves). The equations were solved simultaneously for the various rate constants using MicroMath Scientist software. In addition to the compartmental analysis, various root functions were fitted to the data in order to see if diffusion had played an important role in the kinetics of the adsorption process.[24]

It was frequently seen that a particular adsorption or exchange curve could be fitted well by more than one set of equations. This problem was alleviated by seeking one model which described all curves satisfactorily. Besides, a model was sought which was plausible in terms of the respective mechanism outlined above and both the fitted equivalent circuit and the electrostatic double-layer structure derived previously. Moreover, it was sometimes seen that, even although fits turned out to be reasonable, plausible, and unique, errors in the fitted rate constants were still in the range of tens of percents. As it was unclear to which extent these errors arose from the shortage of the model, from the limited number of radiotracer data, or from statistical scattering of data, no detailed evaluation of errors was made.

Results and Discussion

Fitted Model. Of all two- and three-compartment models fitted, only the model shown in Figure 3a described all data satisfactorily (Figure 3a). The corresponding set of equations which bridge the so-called catenary or serial three-compartment model to the data have been summed up in the Appendix. The model was not only unique but also plausible in terms of the mechanism outlined above and both the fitted equivalent circuit and the electrostatic double-layer structure derived previously.[11,12] The fact that data could be fitted by first-order differential equations (with exponential solutions) rather than by root-type equations implies that the rates of the adsorption processes are ruled by kinetic, electrostatic barriers rather than by mass-controlled, diffusive ones.[11,24] Consequently, the rate

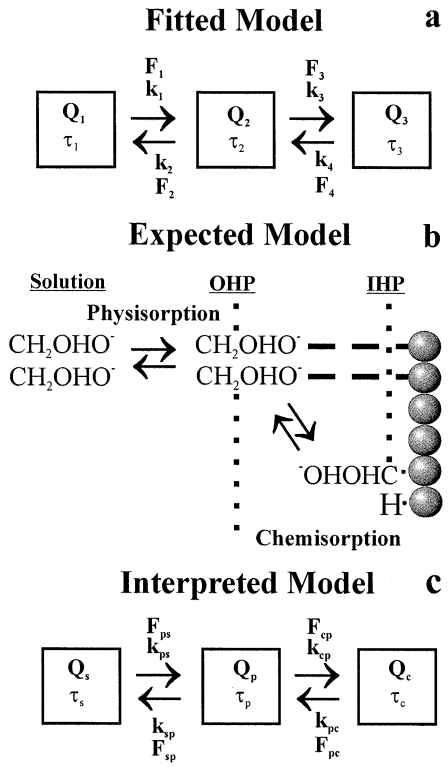

Figure 3. Fitted model which describes the overall adsorption and exchange data best (a). The expected model and the interpreted model were derived from considerations discussed in the text as well as from data obtained by EIS, voltammetry, and DEMS (b and c).[12]

of diffusion or convection was larger than the rate of adsorption when the electrode was held in the up position (adsorption data were collected when the electrode was held in the up position). On the other hand, a very slow, diffusive "random-walk" adsorption seemed to apply to the system when the electrode was held in the down position, as counting rates remained approximately constant under these conditions.[25]

Interpreted Model. The assignments of the fitted mass flows to the actual reaction may be made by bearing in mind the following considerations: First, experiments were carried out in nitrogen-saturated solutions at the OCP, and consequently, diffusion and electron-transfer steps (steps 2, 5, and 7 in the above-given mechanism) may be omitted. Besides, as no hydrogen evolves at the formaldehyde concentrations examined, step 6 may be omitted too.[12] Furthermore, as the pK_a of the weak acidic gem-diol, $CH_2(OH)_2$, amounts to ~13, the gem-diol is largely deprotonated by the alkaline NaOH and the equilibrium of step 1 may be assumed to lie on the right-hand side.[12,15,16] The occurrence of physisorption (step 3) in the reaction has been suggested from our previous studies and from studies reported by Beltowska et al.[5,6,11] The occurrence of chemisorption (step 4) has been indicated by the significant kinetic isotope effect in the reaction and by the presence of dissociated enolate anions at the gold surface, as observed by infrared spectroscopy.[12,26] The adsorption process may therefore be described by the model shown in Figure 3b. Physical assignments to the fitted model can be made by comparing parts a and b of Figure 3, yielding the picture shown in

(22) Godfrey, K. *Compartmental Models and Their Application*; Academic Press: New York, 1983; p 58.
(23) Shipley, R. A.; Clark, R. E. *Tracer Methods for In Vivo Kinetics*; Academic Press: New York, 1972; p 45.
(24) Gileadi, E. *Electrode Kinetics for Chemists, Chemical Engineers and Material Scientists*; VCH Publishers: New York, 1993; p 381.
(25) Laidler, K. J.; Meiser, J. H. *Physical Chemistry*; Houghton Mifflin Company: Boston, 1995; p 881.
(26) Avramov-Ivic, M. L.; Adzic, R. R.; Bewick, A.; Razaq, M. *J. Electroanal. Chem.* **1988**, *240*, 161.

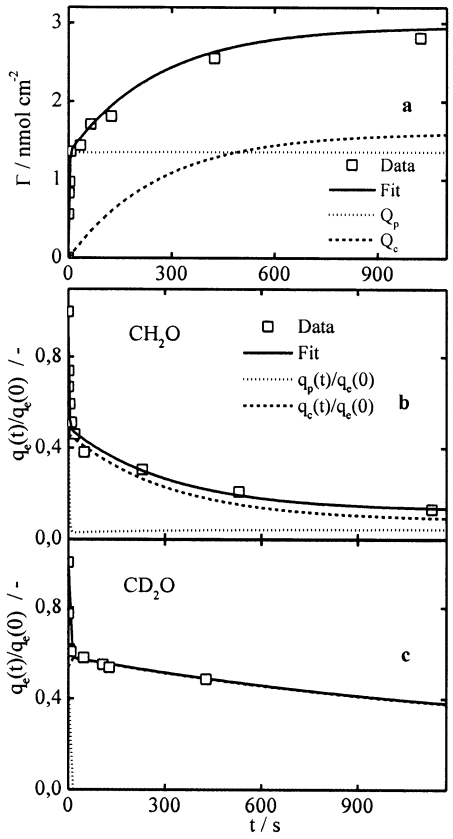

Figure 4. Adsorption of formaldehyde on gold at the OCP in solutions containing 0.1 M NaOH and 0.01 M CH_2O. The fitted analogues and the fitted quantities hosting the chemisorbed and physisorbed states are shown as well (a). Exchange of adsorbed formaldehyde with solute formaldehyde or deuterated formaldehyde together with the fitted analogues (b and c).

Figure 3c.[11,12] Clearly, physisorption and chemisorption of the enolate anion proceed in a catenary fashion rather than in a mammillary one (the enolate anion may then adsorb directly on the gold surface by both physisorption and chemisorption). The model shown in Figure 3c will serve as base for the discussion of the rest of the data.

Adsorption and Exchange Kinetics at the OCP. *Standard Conditions.* The adsorption of formaldehyde on gold at the OCP in a solution containing 0.1 M NaOH and 0.01 M CH_2O (procedure 1, Table 1—standard conditions) is shown, together with the fitted curves, in Figure 4a. The steady state in the adsorption process seems to be reached within ~1000 s, attaining a surface coverage of approximately 50% of the available gold sites, as calculated from a roughness factor of 3, an average Au−Au length of 3 Å, and a "one formaldehyde-to-one gold site" occupation.[27] Analysis of the fitted transition times (Table 2) shows that species spend much more time in the chemisorbed state (τ_c) than in the physisorbed state (τ_p). Besides, the average flow of enolate anions at "infinite" time between the solution and physisorbed state (F_{sp}) is much larger than the average flow between the physisorbed state and the chemisorbed state (F_{pc}). The calculated quantities of species hosting the physisorbed state ($Q_{p,t=\infty}$) and the chemisorbed state ($Q_{c,t=\infty}$) do not differ to a great extent (procedure 1, Table 2 and Figure 4a).

To see if occupation of the gold sites had occurred in a reversible or irreversible manner, the exchange of adsorbed formaldehyde including [^{14}C]-CH_2O with the solute CH_2O (solution 1, Table 1) was studied (Figure 4b). Clearly, such an exchange does occur. The value of 0.13 for the overall fitted residual fraction (Table 3, sum of $q_p(\infty)/q_e(0)$ and $q_c(\infty)/q_e(0)$) does, nevertheless, exceed the value expected for a completely reversible system (this value would be $\sim 10^{-4}$).

Influence of CD_2O. To see if occupation of the gold sites had occurred by a dissociative step (chemisorption) or a nondissociative adsorption step (physisorption), the exchange of formaldehyde (adsorbed from solution 1, Table 1) with deuterated, nonlabeled formaldehyde (solution 2, Table 1) was studied (Figure 4c). Clearly, a pronounced difference in the rate of exchange is observed between CH_2O and CD_2O, confirming the important role of the C−H bond rupture step in the overall adsorption kinetics of the enolate anion (Figure 4b and c).[11,12] Analysis of the fitted curves shows that the difference between CH_2O and CD_2O is more pronounced at longer times, suggesting that another, more rapid step, practically independent of H/D substitution effects, is involved in the kinetics of the adsorption as well. In accordance with the physical assignments outlined above, the slow step is assigned as the chemisorption step whereas the rapid one is assigned as the physisorption step. The transition times obtained from the fits for the exchange curves of CH_2O and CD_2O (procedures 1 and 2 in Table 3) show similar behavior as was observed for the adsorption kinetics under these conditions (Figure 4a): Species prefer to host the chemisorbed state over the physisorbed state.

Residual Fractions. As mentioned, the residual fractions of the exchange curves exceed the values expected for a completely reversible system (Figure 4). This observation may me explained by irreversible adsorption, by an increased background signal due to the incomplete removal of the radioactive solution upon pumping, by insufficient counting statistics, or by the limited measurement time.[14,22] The physical or chemical origin of the nonreversible behavior could nevertheless not be elucidated in detail, as rinsing with water could cause depletion of adsorbed species, and as measurements with the relatively unstable and volatile formaldehyde could be made only for a limited period of time.[15,16] However, as the values of the fitted residual fractions were too large to be explained by insufficient counting rates or incomplete removal of the [^{14}C]-CH_2O containing solution upon pumping (estimated at 0−5% of the initial value), and as these values exceeded the values expected for a completely reversible system by at least a factor of one hundred, the relatively large residual fractions are explained by formation of irreversibly adsorbed species (Figure 4c). This view is further supported by DEMS measurements, which showed D_2 gas evolution at the OCP, and by chronoamperometry, which pointed toward the occurrence of poisoning (irreversible adsorption) at potentials close to the OCP.[12] The gas evolution and poisoning effects were explained by the following side reaction:[12]

$$CD_2OHO^- \rightarrow HCOO^- + D_2\uparrow \qquad \text{(VIII)}$$

The stronger spontaneous, irreversible gas evolution for CD_2O than for CH_2O may be in line with the larger residual fraction for CD_2O than for CH_2O. The large residual fraction may therefore be explained by formation of irreversibly adsorbed formate ions. Compartmental analysis did nevertheless not give straightforward evidence for the occurrence of the irreversible side reaction.

Temperature Dependence. The dependence of the adsorption and exchange of formaldehyde on temperature in solutions containing 0.1 M NaOH and 0.01 M CH_2O

(27) Weast, R. C. *CRC Handbook of Chemistry and Physics*, 66th ed.; CRC Press Inc.: Boca Raton, FL, 1985; p F-87.

Table 2. Fitted Rate Constants (k), State Quantities (Q), Interstate Flows (F), and Transition Times (τ) for the Adsorption Kinetic Curves According to the Model Shown in Figure 3

proc	k_{sp}/s^{-1}	$k_{ps}/10^{-5}\ s^{-1}$	$k_{cp}/10^{-2}\ s^{-1}$	$k_{pc}/10^{-2}\ s^{-1}$	$Q_c(t_\infty)$/nmol	$Q_p(t_\infty)$/nmol	F_{ps}/nmol s^{-1}	F_{cp}/nmol s^{-1}	τ_p/s	τ_c/s
1	0.47	1.92	0.45	0.38	4.72	4.07	1.92	0.02	2.09	262.0
3	2.92	6.58	6.47	2.37	6.14	2.25	6.57	0.15	0.34	42.1
4	3.46	28.2	10.6	41.4	2.08	8.16	28.2	0.86	0.28	2.42
5	1.13	4.96	2.84	5.75	2.16	4.38	4.96	0.12	0.86	17.4
6	4.41	24.2	0.11	2.97	0.20	5.49	24.2	0.01	0.23	33.6
7	1.88	3.62	9.40	4.65	0.07	0.03	0.06	0.01	0.51	21.5

Table 3. Fitted Rate Constants, Residual Fractions, Interstate Flows, and Transition Times (τ) for the Exchange Kinetic Curves According to the Model Shown in Figure 3

proc	k_{sp}/s^{-1}	$k_{ps}/10^{-2}\ s^{-1}$	$k_{cp}/10^{-2}\ s^{-1}$	$k_{pc}/10^{-2}\ s^{-1}$	$q_p(t_\infty)/q_e(0)$	$q_c(t_\infty)/q_e(0)$	τ_p/s	$\tau_c/10^2$ s
1	0.39	2.04	0.57	0.29	0.09	0.042	2.56	3.40
2	0.67	0.15	7.19	0.06	0.26	0.002	1.35	16.6
3	1.06	2.37	4.68	2.93	0.033	0.021	0.90	0.34
4	3.10	1.17	56.6	12.2	0.05	0.005	0.27	0.08
5	0.36	0.18	3.55	6.55	0.003	0.005	2.52	0.15
6	0.84	0.10	532	21.3	0.028	0.001	0.16	0.05
7	1.33	7.68	5.40	9.10	0.031	0.053	0.72	0.11

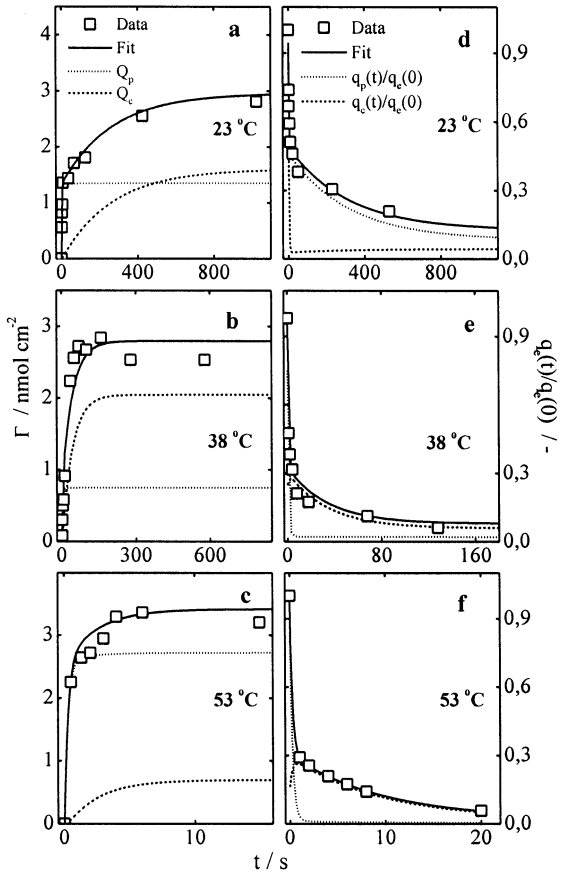

Figure 5. Adsorption kinetics (a−c) and exchange kinetics (d−f) of formaldehyde on gold at different temperatures in solutions containing 0.1 M NaOH and 0.01 M CH_2O, together with the fitted analogues as well as the fitted quantities of species hosting the chemisorbed and physisorbed states (a−f).

(procedures 1, 3, and 4, Table 1) are shown, together with the calculated fits, in Figure 5. A substantial increase in the rate of adsorption and exchange can be observed at higher temperatures. The fitted transition times show too that species spend less time in the physisorbed and chemisorbed states at higher temperatures than at lower temperature (Tables 2 and 3). Examination of the mass flows and rate constants shows that this is a consequence of the increased rate of chemisorption, as the rate of physisorption increases to a lesser extent at higher temperatures. The stronger increase in chemisorption than in physisorption at higher temperatures confirms the view that the E_a of the chemisorption step is ruled to a larger extent by enthalpy terms and to a lesser extent by entropy terms.[12]

Table 4. Derived Activation Energies for the Physisorption and Chemisorption Steps[a]

procedure	E_a^{sp}/kJ mol^{-1}	E_a^{pc}/kJ mol^{-1}
adsorption	62.7	105
exchange	20.4	111

[a] Values were calculated from results shown in Figure 5.

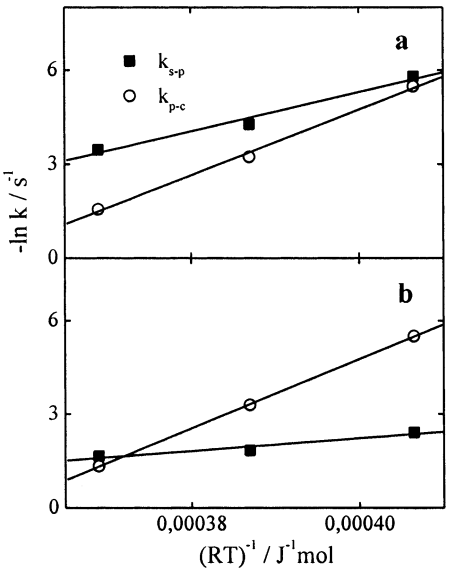

Figure 6. Arrhenius plots of the physisorption and chemisorption steps for the adsorption kinetics (a) and the exchange kinetics (b).

An attempt was made to evaluate the activation energies of the physisorption and chemisorption steps at the OCP by plotting the values of the calculated rate constants at different temperatures (Table 4, Figure 6). Although the results have a low reliability, as only three points could be taken into account, the values obtained suggest that larger activation energies apply to the chemisorption step than to the physisorption step. Besides, the activation energies are large at these OCP conditions, which may be in line with the relatively large overpotentials required to oxidize formaldehyde at significant rates around the OCP.[12]

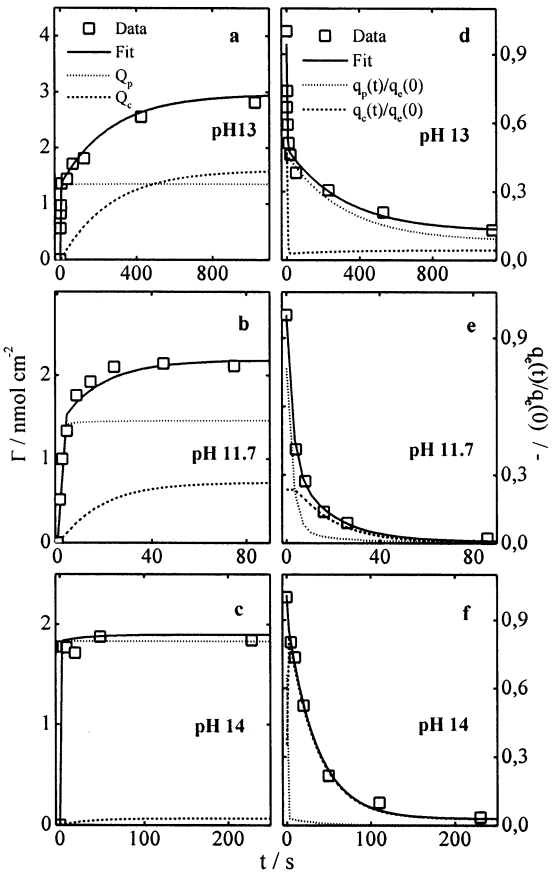

Figure 7. Adsorption and exchange of formaldeyde on gold at different pH in 0.01 M CH_2O solutions together with the fitted curves as well as the fitted quantities hosting the chemisorbed and physisorbed states (a−f).

pH Dependence. The adsorption and exchange of formaldehyde on gold in solutions containing 0.01 M CH_2O and different concentrations of NaOH (procedures 1, 5, and 6, Table 1) are shown, together with the calculated fits, in Figure 7. Clearly, the lowest rates of adsorption and exchange are seen in solutions containing 0.1 M NaOH. Examination of the fits shows that more species occupy the chemisorption than the physisorption state under these conditions (Table 3). The larger occupation of the chemisorption state in solutions containing 0.1 M NaOH than in those containing 0.005 M is explained by the hydroxyl-catalyzed character of the chemisorption step.[5,6] The lower occupation of the chemisorption state in solutions containing 1.0 M than in those containing 0.1 M NaOH is explained by the increased adsorption of hydroxyl ions at the gold surface (Figure 7c). It may support the hydroxyl-mediated adsorption model postulated by Burke et al.[29] The fitting results of the exchange curve at the higher pH do nevertheless contradict this view, as it suggests that species prefer to host the chemisorption state over the physisorption state.

Concentration Dependence. The adsorption and exchange of formaldehyde on gold in solutions containing 0.1 M NaOH and 0.17 mM CH_2O (procedure 7, Table 1) are shown, together with the calculated fits, in Figure 8. Comparison with Figure 4 shows that the adsorption is completed much more rapidly at this low formaldehyde concentration than at 0.01 M. Besides, the enolate anions tend to chemisorb to a greater extent, as revealed by the larger relative quantity of species occupying the chemisorption state.

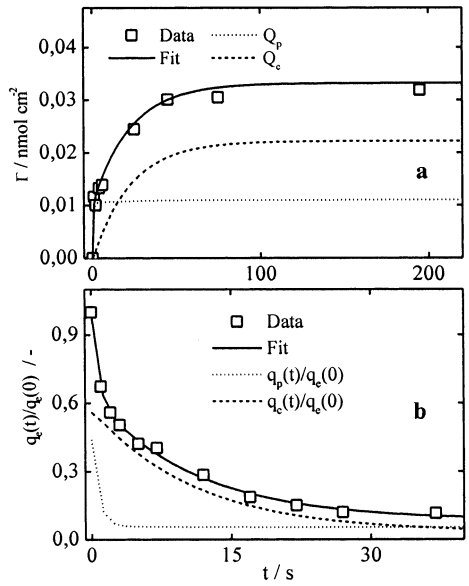

Figure 8. Adsorption and exchange of formaldehyde in 0.17 mM CH_2O solutions together with the fitted curves and the fitted quantities of species hosting the chemisorbed and physisorbed states (a and b).

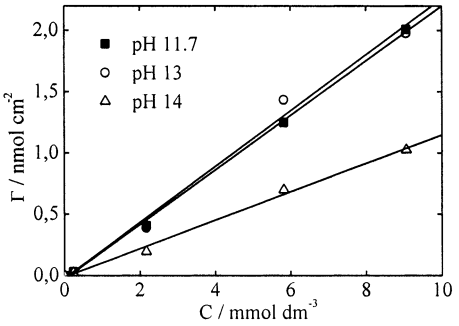

Figure 9. Adsorption isotherms of formaldehyde at the OCP at different pH.

Adsorption Isotherms at the OCP. Adsorption isotherms obtained at the OCP in solutions containing different concentrations of NaOH are shown in Figure 9. The isotherms are linear, implying that adsorbed enolate anions do not inhibit further adsorption of enolate anions. The lower adsorption on gold at the higher pH is in concordance with the adsorption data presented above in Figure 7 and is explained accordingly by increased adsorption of hydroxyl ions at the gold surface. Furthermore, the standard free Gibbs energies, ΔG^*, could be calculated from the initial slopes of the adsorption isotherms using $\Delta G^* = RT \ln K$ (Table 5).[29] Clearly, the lowest Gibbs free adsorption energy is observed at pH 14 although only small differences apply to the various adsorption energies (Table 5). Instead, it was found that the differences in pH manifest in a much more pronounced way in the activation energies of the reaction.[12]

Reaction Kinetics. To study the adsorption and oxidation of formaldehyde under dynamic conditions, a few cyclic voltammograms were recorded in alkaline formaldehyde solutions (Figure 10). A negligible electrooxidation current can be observed for the voltammogram recorded in the solution containing 0.1 M NaOH and 0.1 mM CH_2O. Adsorption does nevertheless seem to occur, as revealed by the decline of the current density associated

(28) Zelanay, P.; Wieckowski, A. *J. Electrochem. Soc.* **1992**, *139*, 2555.
(29) Burke, L. D.; Nugent, P. F. *Gold Bull.* **1997**, *30*, 43.
(30) Gileadi, G. *Electrode Kinetics*; VCH Publishers: New York, 1993; p 403.

Table 5. Free Energies of Adsorption (ΔG_a), Heats of Adsorption (ΔH_a), and Entropies of Adsorption (ΔS_a) Obtained[a]

procedure							
[NaOH]/M	*T*/°C	*V*/V vs OCP	ΔG^*/kJ mol^{-1}	$\Delta G^{\#}$/kJ mol^{-1}	$\Delta H^{\#}$/kJ mol^{-1}	$\Delta S^{\#}$/kJ mol^{-1}	$T\Delta S^{\#}$/kJKmol^{-1}
0.1	22	0	−27.8	−26.8	−9.1	0.06	17.7
0.005	22	0	−27.7				
11.0	22	0	−25.3				
0.1	27	0		−26.4	−20.4	0.02	6.0
0.1	32	0		−26.4	−32.5	−0.02	−6.1
0.1	38	0		−26.8	−48.5	−0.07	−21.8
0.1	43	0		−27.3	−62.1	−0.11	−34.8
0.1	48	0		−27.9	−79.3	−0.16	−51.4
0.1	53	0		−28.7	−93.9	−0.20	−65.2
0.1	22	−1.0	−27.6				
0.1	22	0.55	−27.7				
0.1	22	0.3		−28.0	−36.9	−0.03	−8.9
0.1	27	0.3		−28.3	−37.3	−0.03	−9.0
0.1	32	0.3		−28.5	−37.7	−0.03	−9.2
0.1	38	0.3		−28.7	−38.0	−0.03	−9.3
0.1	43	0.3		−28.8	−38.3	−0.03	−9.5
0.1	48	0.3		−29.0	−38.6	−0.03	−9.6
0.1	53	0.3		−29.1	−38.9	−0.03	−9.8

[a] The values of the OCP have been given in Table 1. All solutions contained 0.1 M CH_2O. ΔG^* and $\Delta G^{\#}$ were obtained from the initial slopes of the adsorption isotherms shown in Figures 9 and 15. $\Delta S^{\#}$ was obtained from the first derivative of the fitted curves shown in Figure 16. $\Delta H^{\#}$ was calculated at each temperature by using $\Delta G^{\#} = \Delta H^{\#} - T\Delta S^{\#}$.

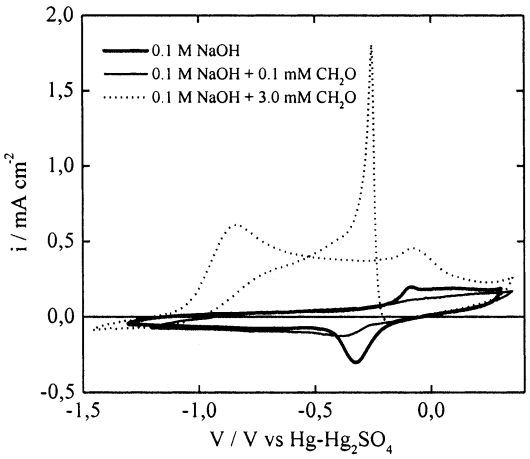

Figure 10. Cyclic voltammograms recorded at a scan rate of 50 mV s^{-1} in different solutions.

with the oxidation and reduction of the gold surface (compare the voltammogram with the one recorded in 0.1 M NaOH).[12] At higher concentration (3.0 mM CH_2O), the oxidation of formaldehyde sets in at −1.2 V versus Hg/Hg_2SO_4 (Figure 10).

The dependence of the current density or rate of the reaction on the scan rate in a solution containing 0.1 M NaOH and 10 mM CH_2O is shown in Figure 11a. The rate of the reaction is affected to a great extent by the scan rate. The linear dependence of the current on the scan rate at voltages below ∼ −0.75 V versus Hg/Hg_2SO_4 confirms the kinetic origin of the overall rate of the reaction at these low potentials (Figure 11b).[12] Interestingly, the value of the KIE (Figure 11c and d) amounts to one at potentials where the electro-oxidation current depends on the scan rate in a linear fashion (∼ −0.75 V vs Hg/Hg_2SO_4). It confirms the view that another step than diffusion (step 2) or chemisorption (step 4) is rate limiting under these conditions.[12] As physisorption (step 3) and desorption of atomic hydrogen are rapid too (steps 6 and 7), and as the equilibrium of step 1 can be assumed to lie on the right-hand side, the rate-limiting step at these potentials is assigned as the desorption of the formate anion.[12] At higher potentials (−0.6 V), the influence of diffusion becomes more apparent, although no Fick behavior applies to the system, as indicated from the absence of linear $v^{0.5}-i$ relationships.[5,6,12] Moreover, the shape of the voltammogram in Figure 11a at 10 mV s^{-1} differs from that of Figure 11c, which is explained by the strong dependence of the inset of oxidation on small fluctuations in nitrogen bubbling rates and poisoning effects.[12] It can be further seen in Figure 11e that no linear Tafel plots apply to the system, confirming the view that the rate-limiting step of the reaction is catalytic or capacitive rather than electrochemical or faradic in nature; that is, the kinetics of the reaction cannot be described by an exponential Butler−Volmer-type equation.[11]

Potential Dependence of Adsorption. The adsorption of formaldehyde in solutions containing 0.1 M NaOH and different concentrations of formaldehyde is shown in Figure 12a. The almost constant adsorption with increasing potentials (Figure 12b) points toward a constant ratio between the rate of adsorption and the rate of desorption of species. The absence of depletion of carbon species at the gold surface under conditions where diffusion rules the overall rate of the reaction suggests that adsorbed species leave the surface upon the approach of reactants rather than upon changes in the electrode potential. Besides, the strong dependence of the surface coverage on the formaldehyde concentration and the invariance of the adsorption isotherms with increasing potentials (see below) also support the view that potential gradients on the solution side are more important in the adsorption of species than the potential of the electrode. These observations are in concordance with the electrostatic picture derived by EIS, which implied that much larger potential gradients apply between the IHP and the solution than between the gold surface and the IHP.[11]

Quantitative insight into the dependence of the quantity of species adsorbed on the formaldehyde concentration was obtained by plotting the adsorption isotherms at different potentials (Figure 13a). The ΔG values obtained from the slopes are potential invariable, confirming the view that the electrode potential affects the E_a between the various states rather than the (relative) value of the Gibbs energies (Table 5).[12] Moreover, the dependence of the reaction rate on the formaldehyde concentration and the quantity of species adsorbed (Γ) yielded linear "$i-\log C$" and "$i-\log \Gamma$" plots (Figure 13b and c), from which the reaction orders in C and Γ could be derived (Table 6). Up to −0.15 V, the orders approach the value of one which

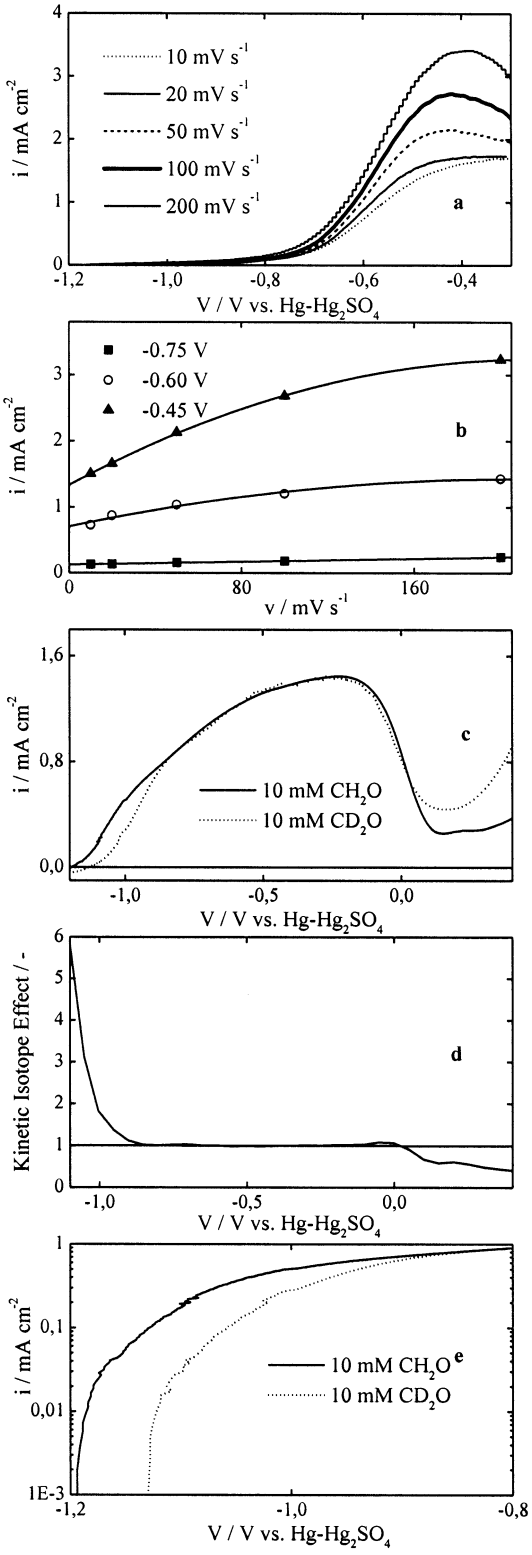

Figure 11. Linear sweep voltammograms recorded at different scan rates in solutions containing 0.01 M CH_2O and 0.1 M NaOH (a). Dependence of the current density on the scan rate at three different potentials (b). The linear sweep voltammograms recorded in a solution containing 0.1 M NaOH and 0.01 M CH_2O and in one containing 0.1 M NaOH and 0.1 M CD_2O show a significant KIE at low and high potentials (c, d). The voltammograms were not characterized by a linear Tafel slope (e).

is in concordance with results published by Beltowska et al.[5,6] (Table 6). At higher voltages, the oxidation of the gold surface sets in and lower reaction orders are obtained.

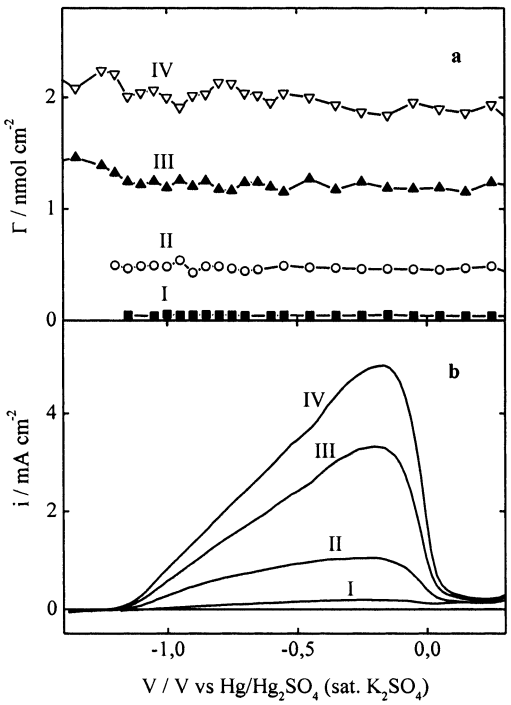

Figure 12. Adsorption of formaldehyde at different potentials in a solution which contained 0.1 M NaOH and 0.22 mM CH_2O (I), 2.41 mM CH_2O (II), 5.82 mM CH_2O (III), and 9.06 mM CH_2O (III), respectively (a). The current densities were obtained at a scan rate of 10 mVs^{-1} (b).

The adsorptions of formaldehyde on gold in solutions containing 0.005 M NaOH and different concentrations of formaldehyde are shown in Figure 14a. Some irregular features are observed at higher concentrations, of which the origin is not clear. The electro-oxidation current, recorded at a sweep rate of 10 mV s^{-1}, does not trace the adsorption (Figure 14b), which is explained in the same fashion as above for solutions containing 0.1 M NaOH. Furthermore, the quantity of species adsorbed is slightly lower in 0.005 M NaOH than in 0.1 M NaOH whereas the current is much lower. It suggests that the role of hydroxyl ions in the rate of adsorption is less apparent than the stoichiometric role of the hydroxyl ions in the rate of the overall reaction.

The adsorptions of formaldehyde on gold in solutions containing 1.0 M NaOH and different concentrations of formaldehyde are shown in Figure 15a. A local minimum around the OCP and a maximum at −0.7 V can be observed at the highest formaldehyde concentration. The maximum at −0.7 V coincides with the crossing of the various voltammograms. Below this voltage, poisoning (irreversible accumulation of species) of the gold surface seems to occur, as witnessed by the increasing coverage (Figure 15a). Above this voltage, the irreversibly adsorbed species may be oxidized.[12]

Temperature Dependence of Adsorption. The adsorption of formaldehyde at different temperatures in solutions containing 0.1 M NaOH and either 10 mM CH_2O or 0.17 mM CH_2O is shown in Figure 16a and b. An increase in the adsorption is observed at higher temperatures at the OCP for both solutions whereas a smaller increase applies to the adsorption at 300 mV versus the OCP. The stronger increase in adsorption at the OCP than at 300 mV is in line with the lower relative rate of chemisorption (larger value of the KIE) at the OCP than at 300 mV, as the E_a of the rate-limiting chemisorption step is dominated by the enthalpy.[12] At 300 mV versus the OCP, the more entropy-controlled desorption of the

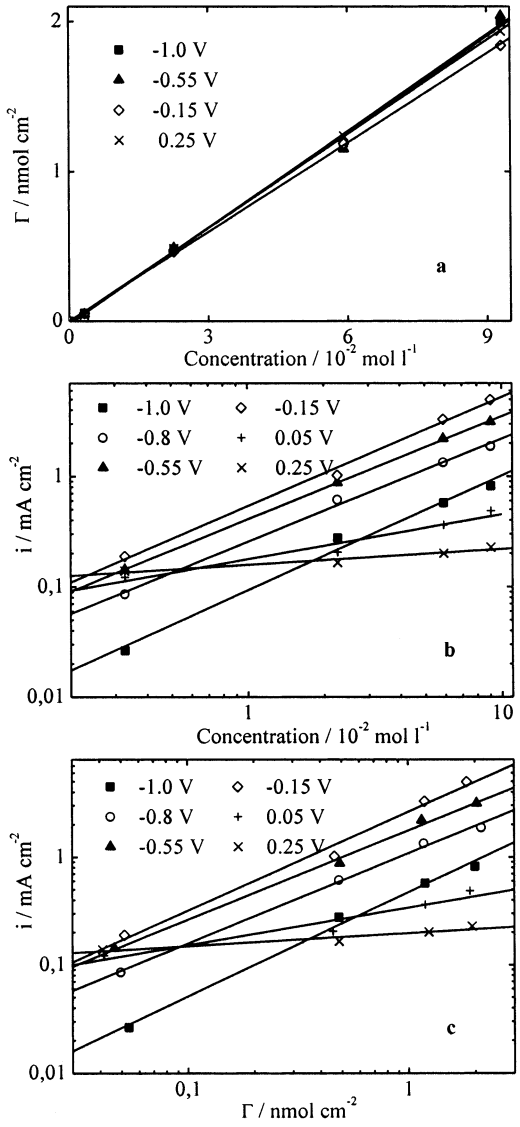

Figure 13. Adsorption isotherms at different voltages in solutions containing 0.01 M CH_2O (a). Dependencies of the current densities on the concentration and on the quantity of species adsorbed at the electrode (b and c).

Table 6. Reaction Orders Obtained in the Concentration (n_c) and Surface Concentration (n_Γ) for Solutions Containing 0.1 M NaOH and 0.01 M CH_2O

V/V vs Hg_2SO_4	n_C	n_Γ
−1.0	1.04	0.97
−0.55	0.94	0.83
−0.15	0.99	0.92
0.25	0.41	0.12

formate ion may become more important in the kinetics of the reaction, favoring a smaller increase.[12]

Adsorption isotherms were constructed from the three concentrations considered, that is, 10, 0.17, and 0.0 mM CH_2O, through which linear isotherms could be fitted with correlation factors larger than 0.99. The free energies of adsorption ($\Delta G_a^{\#}$) were derived from the slopes of these isotherms at different temperatures (Table 5). A value of −26.8 kJ mol^{-1} was obtained at the OCP and at room temperature, which was in reasonable agreement with the value found above for the adsorption isotherms at the OCP (−27.8 kJ mol^{-1}). Both values are much larger than those reported in the literature for the conversion of nonhydrated formaldehyde to formate (−103 kJ mol^{-1}),

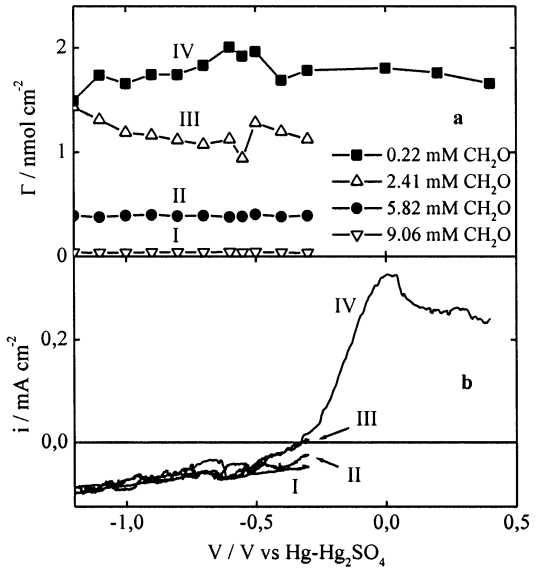

Figure 14. Adsorption of formaldehyde at different potentials in solutions which contained 5 mM NaOH and 0.22 mM CH_2O (I), 2.41 mM CH_2O (II), 5.82 mM CH_2O (III), and 9.06 mM CH_2O (IV), respectively (a). The corresponding current densities were recorded at a scan rate of 10 mVs^{-1} (b).

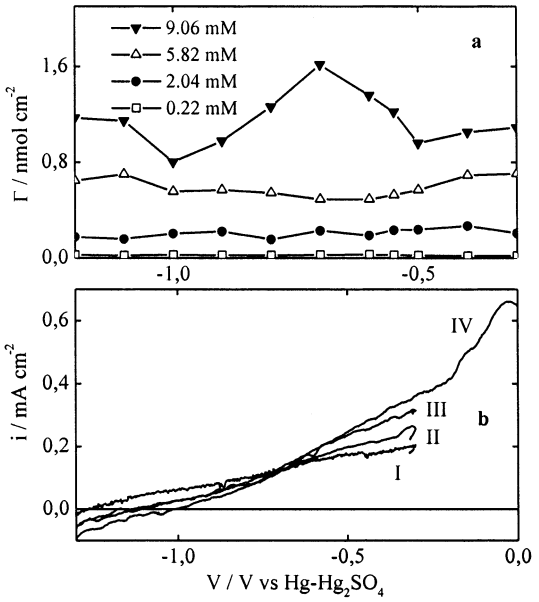

Figure 15. Adsorption of formaldehyde at different potentials in solutions which contained 5 mM M NaOH and 0.22 mM CH_2O (I), 2.41 mM CH_2O (II), 5.82 mM CH_2O (III), and 9.06 mM CH_2O (IV), respectively (a). The corresponding current densities were recorded at a scan rate of 10 mV s^{-1} (b).

suggesting that solution effects affect the thermodynamics of the system substantially.[27]

The dependence of the ΔG values on temperature obeyed a linear relationship at 300 mV whereas a second-order relationship ($\Delta G_a^{\#} = -411.2 + 2.54T - 0.004T^2$) was found at the OCP (Figure 16c). Free heats of adsorption (ΔH_a) and free entropies of adsorption (ΔS_a) could be derived at different temperatures from the first derivatives of the fitted polynomes and by using $\Delta G_a^{\#} = \Delta H_a - T\Delta S_a$ (Figure 16c and Table 5). It can be seen that the values of ΔH_a and ΔS_a do not depend to a great extent on the temperature for data obtained at 300 mV. On the other hand, a significant increase is seen in ΔH_a and ΔS_a at the OCP. The values of $T\Delta S_a$ give an indication for the contribution of the entropy to the Gibbs free energy of adsorption at

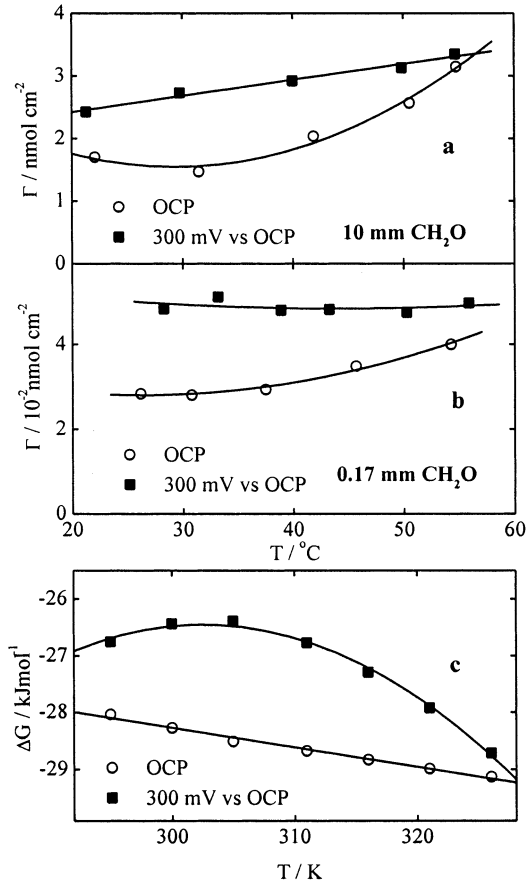

Figure 16. Adsorption at different temperatures and potentials in solutions which contained 0.1 M NaOH and 10 mM CH_2O (a) and 0.17 mM CH_2O, respectively (b). The Gibbs free energies could be derived at different temperatures from the adsorption isotherms which were constructed from the data presented in parts a and b. See text for further explanation (c).

a specific temperature (Table 5). In most cases, the enthalpy tends to make the overall reaction exothermic whereas the entropy tends to make it endothermic

Kinetic and Thermodynamic Model. As mentioned, a semiquantitative kinetic model was proposed which described the reaction at potentials around the OCP in a semiquantitative manner.[11,12] The model consisted of three (pseudo)stable states, that is, the solution, the OHP, and the IHP, which were interconnected by two energy humps. The model can be specified by taking into account the results and considerations discussed above. Different diagrams can be constructed for different cases (Figure 17):

The energy diagram obtained for the adsorption under steady-state conditions at 25 °C is shown in Figure 17a. The activation energies associated with the transitions between the various states have been taken from Table 4; the Gibbs energies, the heats of adsorption, and the entropies of adsorption have been taken from Table 5. The value of the energy representing the OHP and IHP has been calculated from the Gibbs energies by assuming that the ratio of the energy of the IHP and the OHP is equal to the ratio of the transition times of species in the IHP and OHP (Table 3). It is clear from Figure 17a that the energy hump associated with the transition between the IHP and the OHP is largest and that the Gibbs free energy of the overall reaction consists mainly of a positive entropy term. The situation is different under dynamic conditions at the OCP, as witnessed by a larger hump associated with the transition of the enolate anion to the

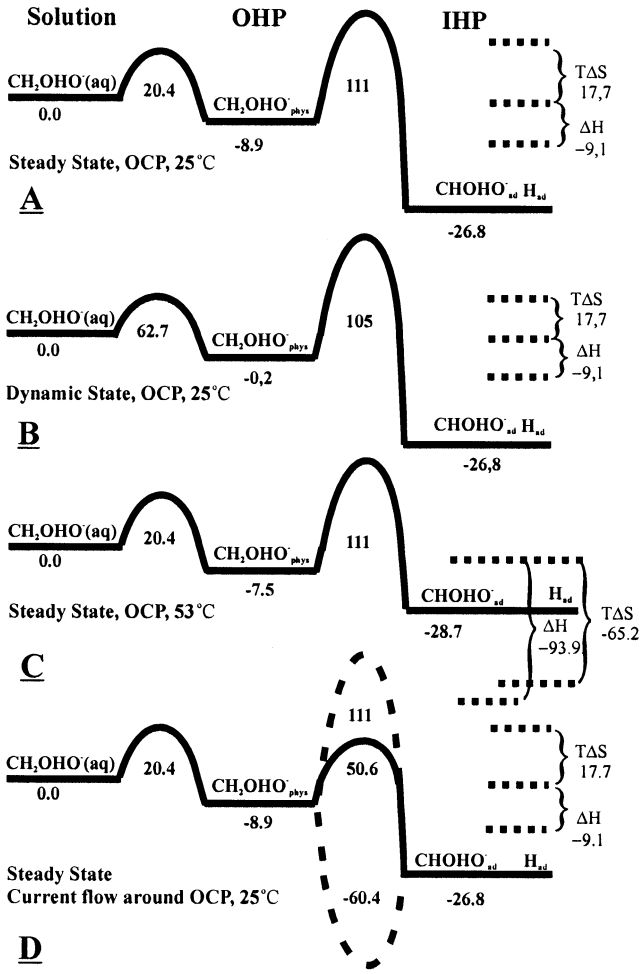

Figure 17. Reconstruction of the energy diagrams of the reaction under different conditions. The numbers reflect the values of the energies in kJ mol^{-1} (a−d).

OHP and a slightly larger one with the transition of the enolate anion to the IHP. Besides, the level of the OHP is somewhat lifted (Figure 17b).

At 53 °C, both the enthalpy of adsorption and entropy of adsorption decrease drastically (Figure 17c). In this case, the Gibbs free energy of the overall reaction is dominated by the enthalpy. Besides, the state corresponding with the IHP is raised relative to the one corresponding with the OHP. At potentials close to the OCP, the oxidation of the adsorbed, dissociated enolate anions at the gold surface sets in and the situation changes drastically (Figure 17d). Namely, the net activation energy is lowered as a result of the rather large entropy contribution associated with the desorption of the formate anion.[12] The negative contribution dominates at potentials sligthly larger than the OCP, resulting in negative capacitive or inductive loops in the impedance spectra.[11] As mentioned, the Gibbs free energy of the overall reaction does not alter under these conditions.

Summary

Adsorption, exchange, and oxidation of formaldehyde have been studied on gold at various potentials, temperatures, pH's, and concentrations by the radiotracer thin-gap method. On the basis of this study, and of the results from EIS, voltammetry, chronoamperometry, and DEMS presented in two previous reports,[11,12] the most important observations, results, and considerations are summed up:

(1) The adsorption of formaldehyde at the OCP proceeds in a serial fashion with two reversible rates of adsorption: a rapid physisorption and a slow chemisorption. The adsorption isotherms are approximately linear at concentrations below 10 mM formaldehyde.

(2) At pH 13, the electro-oxidation of formaldehyde to formate is approximately first-order in the concentration of formaldehyde and in the quantity of species adsorbed at the gold surface.

(3) At pH 13, the rate of the overall electro-oxidation reaction is likely ruled by chemisorption of the enolate anion at low potentials (−1.1 V vs Hg/Hg_2SO_4), by desorption of formate at medium potentials (−0.9 to −0.7 V vs Hg/Hg_2SO_4), and by the diffusion of reactants and products at the highest potentials (> −0.5 V vs Hg/Hg_2SO_4).

(4) The value of ΔG of the overall electro-oxidation reaction is much larger in solution than the theoretical value in a vacuum (−27.8 vs −103 kJ mol^{-1}), suggesting that the solution affects the thermodynamics of the reaction substantially. The value of ΔG does not depend to a great extent on the potential, temperature, and pH. The E_a is strongly affected by these parameters.

(5) The enthalpy of the reaction tends to make the reaction exothermic whereas the entropy tends to make it endothermic in most cases. At 22 °C and at the OCP, the ΔG consists mainly of positive entropy. At 53 °C, ΔG is dominated by the negative enthalpy.

(6) The E_a of the chemisorption step in the reaction is dominated by the enthalpy. The E_a of the desorption of species is ruled by the entropy.[12]

(7) ΔG_a ranges between −29.1 and −26.4 kJ mol^{-1}, ΔH_a ranges between −93.9 and −9.1 kJ mol^{-1}, and ΔS_a ranges between −0.2 and 0.1 kJ mol^{-1}.

(8) The strong dependence of the quantity of species adsorbed on the formaldehyde concentration and the invariance of the adsorption isotherms with increasing potentials are in line with the view that potential gradients on the solution side are more important in the adsorption of species than the potential of the electrode itself.[11]

(9) The kinetics and thermodynamics of the reaction can be described under different conditions by one physical model. In this model, the enolate anion diffuses to the reaction center, followed by reversible physisorption, reversible chemisorption, irreversible oxidation, and desorption of reaction products (hydrogen, water, and formate). The model conceives the reaction by three stable states, that is, the solution, the OHP, and the IHP, which are interconnected by two energy humps. A kinetic description of simple electroless processes may be accomplished by implementing metal ions in the model, and the pursued springboard for an overall kinetic description of electroless processes has therefore been set.

Acknowledgment. The authors are indebted to M. Fraai and T. G. Verburg for assistance in the measurements and fitting procedures, respectively. Prof. A. Wieckowski, Dr. A. Kolics, and Dr. A. Thomas are acknowledged for assistance in setting up the equipment for the radiotracer experiments.

Appendix

Adsorption Experiments. A closed, catenary three-compartment model (Figure 3a) has been used for fitting the adsorption data. It can be described by a system of three differential equations:

$$dQ_s(t)/dt = k_{sp}Q_p(t) - k_{ps}Q_s(t) \quad \text{(A1)}$$

$$dQ_p(t)/dt = k_{ps}Q_s(t) + k_{pc}Q_c(t) - k_{sp}Q_p(t) - k_{cp}Q_p(t) \quad \text{(A2)}$$

$$dQ_c(t)/dt = k_{cp}Q_p(t) - k_{pc}Q_c(t) \quad \text{(A3)}$$

with

$$Q_e(t) = Q_p(t) + Q_c(t)$$

where the quantity of unlabeled material (tracee) in a compartment is denoted as Q.[23] Q_s, Q_p, and Q_c represent the quantities (in nmol) in the solution, in the physisorbed, and in the chemisorbed state, respectively, with the initial compartment quantities $Q_s(0) = 100\,000$ nmol (procedures 1−6) or 1710 nmol (procedure 7), and $Q_p(0) = 0$ and $Q_c(0) = 0$. The $Q_e(t)$ values were obtained from $\Gamma(t)_e$ by using

$$Q_e(t) = \Gamma(t)_e RA \quad \text{(A4)}$$

where $\Gamma(t)_e$ is the surface concentration (nmol per real cm^2), R is the roughness factor (−), and A is the geometrical area of the electrode (cm^2).

The rate of transfer (flow) of tracee is denoted as F (in nmol s^{-1}); F_{ps} represents the flow to the physisorbed state from the solution. Likewise F_{sp}, F_{pc}, and F_{cp} represent the flows to the solution from the physisorbed state, to the physisorbed state from the chemisorbed state, and to the chemisorbed state from the physisorbed state, respectively. The rate constant is denoted as k (s^{-1}). The flows in steady state ($t = \infty$, $Q(\infty) =$ constant) between the compartments can be obtained from

$$F_{ps}(\infty) = F_{sp}(\infty) = k_{ps}Q_s(\infty) = k_{sp}Q_p(\infty) \quad \text{(A5)}$$

$$F_{pc}(\infty) = F_{cp}(\infty) = k_{pc}Q_c(\infty) = k_{cp}Q_p(\infty) \quad \text{(A6)}$$

The transition times in the compartments can be obtained from

$$\tau_s = 1/k_{ps} \quad \text{(A7)}$$

$$\tau_p = 1/(k_{sp} + k_{cp}) \quad \text{(A8)}$$

$$\tau_c = 1/k_{pc} \quad \text{(A9)}$$

Exchange Experiments. The exchange experiments are, in contrast with the adsorption experiments, initially in steady state: $dQ(t)/dt = 0$. In this case, the radiotracer quantity (q_e) on the electrode was measured and fitted. The fractional loss of tracer from the physisorbed and chemisorbed state can be described by

$$d[q_p(t)/q_e(0)]/dt = k_{ps}q_s(t)/q_e(0) + k_{pc}q_c(t)/q_e(0) - k_{sp}q_p(t)/q_e(0) - k_{cp}q_p(t)/q_e(0) \quad \text{(A10)}$$

$$d[q_c(t)/q_e(0)]/dt = k_{cp}q_p(t)/q_e(0) - k_{pc}q_c(t)/q_e(0) \quad \text{(A11)}$$

Likewise

$$d[q_s(t)/q_e(0)]/dt = k_{sp}q_p(t)/q_e(0) - k_{ps}q_s(t)/q_e(0) \quad \text{(A12)}$$

$$q_e(t)/q_e(0) = q_p(t)/q_e(0) + q_c(t)/q_e(0) \quad \text{(A13)}$$

The initial values for the physisorbed and chemisorbed states were obtained from the adsorption experiments at $t = \infty$: $q_p(0)/q_e(0) = Q_p(\infty)/Q_e(\infty)$, $q_c(0)/q_e(0) = Q_c(\infty)/Q_e(\infty)$ and $q_p(0)/q_e(0) + q_c(0)/q_e(0) = 1$, while $q_s(0)/q_e(0) = 0$.

The system of differential equations was simultaneously solved for the four rate constants.

LA010572C